Atomic-layer-deposited Al_2O_3 on Bi_2Te_3 for topological insulator field-effect transistors

Han Liu and Peide D. Ye[a)]
School of Electrical and Computer Engineering and Birck Nanotechnology Center, Purdue University, West Lafayette, Indiana 47907, USA

(Received 22 April 2011; accepted 5 July 2011; published online 4 August 2011)

We report dual-gate modulation of topological insulator field-effect transistors (TI FETs) made on Bi_2Te_3 thin flakes with integration of atomic-layer-deposited (ALD) Al_2O_3 high-k dielectric. Atomic force microscopy study shows that ALD Al_2O_3 is uniformly grown on this layer-structured channel material. Electrical characterization reveals that the right selection of ALD precursors and the related surface chemistry play a critical role in device performance of Bi_2Te_3 based TI FETs. We realize both top-gate and bottom-gate control on these devices, and the highest modulation rate of 76.1% is achieved by using simultaneous dual gate control. © *2011 American Institute of Physics*. [doi:10.1063/1.3622306]

Three dimensional topological insulator (TI) materials, such as Bi_2Te_3, Bi_2Se_3, and Sb_2Te_3, have recently attracted much attention due to their unique physical properties.[1–5] These structures are layered like graphene but appear to behave like insulators having a band gap in the material bulk. However, these materials show metallic behavior on their surfaces. The surface states of TIs consist of an odd number of massless Dirac cones, around which the linear dispersion of the electron spectrum is such that the carriers reach extremely high surface carrier mobilities up to 9000-10 000 cm^2/Vs.[6] Moreover, these surfaces, protected by time reversal symmetry,[7] result in a non-scattering carrier transport regime, making TIs rather promising for future nanoelectronics applications with ultralow power dissipation.

In order to realize practical TI field-effect transistors (FETs), it is important to study the integration of gate dielectrics on these materials so that the channel current can be controlled by the top-gate. In some early studies of Bi_2Te_3 based TI devices, where a heavily doped silicon back gate was used, no modulation was observed within a back-gate voltage sweep from −50 V to 50 V at room temperature.[8] The highest modulation obtained is around 20% measured at less than 10 K.[9] For Bi_2Se_3, which has a larger bandgap of 0.3 eV than 0.14 eV of Bi_2Te_3, minuscule gate modulation was reported using top-gate control at room temperature,[10] while much larger modulation was achieved by the back-gate sweeps.[11] Although these are inspiring results to observe the field effect by using a global back-gate, this cannot satisfy the requirement for real device applications, which requires individual device top-gate control and room temperature operation. Therefore, the realization of highly efficient top-gate modulation for Bi_2Te_3 and other TI materials at room temperature is urgently needed.

In this letter, we demonstrate Al_2O_3 growth by atomic-layer deposition (ALD) with two different precursors on Bi_2Te_3 top surfaces. The uniformity of the surface morphology after the ALD Al_2O_3 deposition is also studied. Electrical characterization has shown a strong modulation of Bi_2Te_3 based TI FETs with both top-gate and back-gate controls. Bi_2Te_3 thin flakes were peeled off from bulk ingots by standard 3M scotch tape techniques[12] and were then transferred to a highly doped silicon wafer with 300 nm thick SiO_2. The thickness of these ultrathin flakes is less than 50 nm. Ten nanometer Al_2O_3 high-k dielectric layers were deposited by an ASM F-120 ALD system at 200 °C by using tri-methyl-aluminum (TMA) and H_2O or TMA and O_3 as precursors. The pulse time is 0.8 s TMA and 1.2 s H_2O, or 1s TMA and 1 s O_3, and the purge time is 6 s N_2 for each precursor. Source/drain regions were defined by optical lithography. Al_2O_3 was etched away using buffered oxide etch (BOE) at these source/drain regions, followed by e-beam evaporation of a 20 nm/40 nm Cr/Au metal and lift-off process for ohmic contacts. A 10 nm/50 nm Cr/Au layer was finally deposited as the top-gate. Final device structure is shown in Figure 1(a), which is similar to a traditional metal-oxide-semiconductor FET, but with two conducting surfaces and one conducting bulk channel in the channel region.

The crystal structure of Bi_2Te_3 has been shown to be similar to graphene, with stacking layers bonded by the Van der Waals force. The lattice constant for hexagonal Bi_2Te_3 is 0.4384 nm for the a-axis and 3.045 nm for the c-axis.[13–16] Each layer of Bi_2Te_3, a quintuple layer with the thickness of ~1 nm, consists of the five layer sequence Te-Bi-Te-Bi-Te. Three quintuple layers form one unit cell.[8] On the top and bottom Te layers, there are no dangling bonds at the surface. This may lead one to suspect that it is not possible to deposit ALD Al_2O_3 directly on these flakes because there would be no chemical absorption due to the absence of dangling bonds at surface, as generally seen in the case of graphene. Early studies also revealed that ALD Al_2O_3 fails to be deposited on graphene surfaces but would only cluster and grow on graphene edges and ultimately form nanoribbons.[17,18] However, our results show that this problem does not occur for Bi_2Te_3. A Veeco Dimension 3100 AFM was used to study the flake surface and the layer edges after Al_2O_3 deposition. The pristine Bi_2Te_3 surface was studied after peeling and being transferred to SiO_2/Si substrates. We notice the surface is not as smooth as the graphene surface. This might be attributed to the fact that Bi_2Te_3 is not as highly air-stable as

[a)]Author to whom correspondence should be addressed. Electronic mail: yep@purdue.edu.

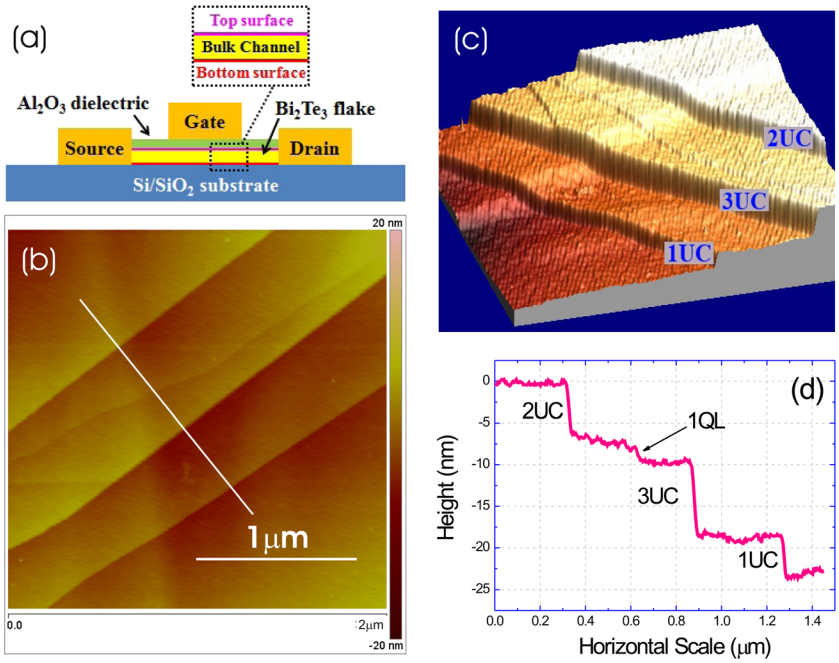

FIG. 1. (Color online) (a) Schematic device structure of a Bi_2Te_3 based TI FET. (b) AFM image of Bi_2Te_3 surface with multiple quintuple layer terraces coated with an ultrathin ALD Al_2O_3 layer. (c) Three-dimensional profile of the same surface showing different thicknesses of the broken layers with 1-3 unit cells. (d) AFM height measurement of the smooth terraces along the white line illustrated in Figure 1(b).

graphene; oxygen and water molecules in air can slightly oxidize the Te-terminated surface. This oxidation facilitates the following ALD process by creating nucleation spots for precursor absorption. The smallest step observed is ~1 nm corresponding to the thickness of one quintuple layer. Most of terraces have the heights of single or multiple unit cells. Figure 1(b) shows the surface morphology of Bi_2Te_3 surface after 20 cycles of ALD growth using TMA and H_2O, corresponding to ~1.8 nm Al_2O_3 deposition. In the graphene case, the surface of graphene remained intact while Al_2O_3 nanoribbons are clearly formed at the graphene edges.[17] No Al_2O_3 nanoribbons or clusters can be observed at the Bi_2Te_3 layer edges. Figure 1(c) shows that ALD Al_2O_3 is conformal and uniformly coated on a series of steps of the peeled Bi_2Te_3 surface with the relative step height remaining similar before ALD. Figure 1(d) shows the measured heights of ~ 3 nm, 9 nm, and 6 nm corresponding to 1–3 unit cells. These observations show that the π-bond in pristine Bi_2Te_3 is not chemically inert in atmosphere as graphene. This instability makes direct ALD growth of dielectrics on such layered structures possible; however, the surface reactions definitely induce potential defects at the high-k/TI interface and hence deteriorate device performance as well.

Electrical characterization was performed after device fabrication using a Keithley 4200. Two devices, one using TMA/H_2O (Device 1) and another using TMA/O_3 (Device 2) as precursors for Al_2O_3 are studied here. The typical geometric features are 2 μm in gate length and 1 μm in gate width. The channel resistance, including the contact resistance, for Devices 1 and 2 are 32 kΩ and 25 kΩ, respectively, indicating that the flake thicknesses are similar. Linear I-V characteristics indicate a good ohmic contact to the Bi_2Te_3 flakes. Figures 2 shows independent top-gate and back-gate modulation for both devices with another gate floating. The top-gate and back-gate leakage currents are less than 10^{-10} A. We do not observe an electron-hole or ambipolar transition because the strong stoichiometric doping of Bi_2Te_3 makes it an n-type material with an estimated doping concentration of ~10^{19}/cm^3. For Device 1, a maximum of 45.6% modulation is reached through back-gate control, where the back-gate voltage is swept from −50 V to 50 V. We calculate the transconductance (g_m) to be 9.8 nS. Comparatively, the top gate g_m is measured 60 nS at its maximum, six times larger than the back-gate g_m due to the thinner top dielectric thickness and higher k value. Though we get an improved value for transconductance by top-gate control, the improvement is not as high as we expect considering the oxide thickness and dielectric constant for both SiO_2 as back-gate oxide and Al_2O_3 for top-gate oxide. The top-gate g_m should be around 60 times larger than back-gate g_m, if we don't consider top-gate partial coverage of the channel and roughly estimate the practical dielectric constant of Al_2O_3 to be ~7.8, twice as that of SiO_2. The stark contrast between predicted and measured values indicates non-ideal Al_2O_3/Bi_2Te_3 interfaces, which is consistent with the discussions above. Also, from the extrinsic transconductances, we can estimate the low limit of the effective electron mobility with top-gate control to be ~1.69 cm^2/Vs and with back-gate control to be ~17.0 cm^2/Vs. This effective mobility contains two parts, the surface state mobility and the bulk mobility. The results indicate that the low mobility bulk channel is the dominant conducting channel and the high mobility surface channels are degraded by the poor interfaces, in

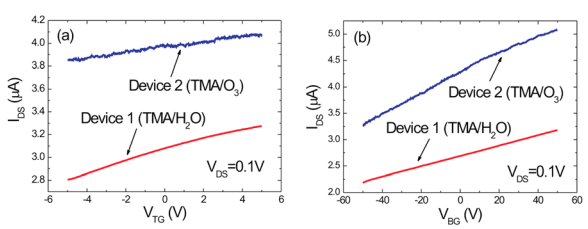

FIG. 2. (Color online) (a) Drain current vs top-gate bias of two Bi_2Te_3 TI FETs with a 10 nm Al_2O_3 as top-gate dielectric; (b) drain current vs back gate bias of the same devices with a 300 nm SiO_2 as back-gate dielectric. Drain-source voltage is 0.1 V in both measurements. The observed minor drain current change at the same bias condition is ascribed to the change of contact resistance and interface traps after gate bias stress.

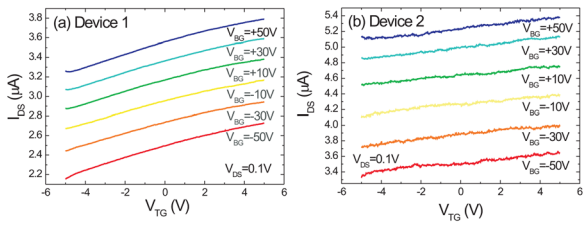

FIG. 3. (Color online) Drain current vs dual gate modulation of two Bi_2Te_3 TI FETs. (a) Bi_2Te_3 TI FET with a 10 nm Al_2O_3 deposited by TMA and H_2O and (b) Bi_2Te_3 TI FET with 10 nm Al_2O_3 deposited by TMA and O_3.

particular, the top interface. Poor interface conditions easily result in a strong degradation of field-effect modulation efficiency as demonstrated in ALD high-k/III-V MOSFETs.[19] Compared to III-V MOSFETs, such interface degradation in Bi_2Te_3 could impose more serious problems in device performance due to its unique carrier transport properties. It has been stated in previous studies that the conductance of those topological insulators is composed of two parts: the bulk conductance and the surface conductance, including the top surface conductance and bottom surface conductance.[10] The two surface conducting channels are of interests due to its high mobility and non-scattering carrier transport. Considering the large intrinsic carrier density in its bulk, the top surface is more sensitive to the top gate control than the bottom surface, so the two surfaces do not play symmetric roles under gate bias. The bottom surface has a better interface condition with the back SiO_2 dielectric as it has been left intact during the fabrication process, resulting in better back-gate control at the same electrical field. However, the top surface condition of the flakes had been changed to some extent due to Al_2O_3 deposition, reacting with H_2O at 200 °C.[20] This reaction might not be severe enough to completely damage the material, as there was only a tiny trace of water vapor as one precursor in one of the alternating ALD pulses. In addition, this water corrosion could only take place in the first several cycles of Al_2O_3 deposition and would naturally cease when the flake is covered with Al_2O_3. But then again, the water corrosion could considerably impact on the interface quality, resulting in a significant decrease in surface modulation under field-effect.

In the same Figures 2(a) and 2(b), the counterparts of top-gate and back-gate control of Device 1 are also shown. Compared to Device 1, Device 2 shows similar back-gate control, with a maximum modulation of 55.8% for a gate sweep of −50 V to 50 V. However, the two devices differ in top-gate control. Device 1 has a maximum modulation of 16.7% with a smoother curve, whereas Device 2 has a modulation of only 5.9% with a noisier curve, with the top-gate voltage ranging from −5 V to 5 V. The weaker top gate modulation in Device 2 further supports our conclusion that ALD precursors are chemically absorbed to the top surface of Bi_2Te_3. In Device 2, the use of ozone as an oxidant ALD precursor leads to greater top surface damage during the first several cycles of ALD growth because ozone is a stronger oxidant than H_2O. As a consequence, the top interface of Device 2 is more defective and the top-gate shows weaker channel modulation and much noisy curves.

Finally, the simultaneous dual gate modulations of Bi_2Te_3 are shown in Figure 3. The top gate voltage is swept from −5 V to 5 V while the back gate ranges from −50 V to 50 V with a 20 V step. We achieve the highest modulation rate of 76.1% for Device 1 and 61.8% for Device 2. All these indicate a significant enhancement in modulation for Bi_2Te_3 thin flakes at room temperature, using Al_2O_3 high-k as a top-gate dielectric and dual gate control. Development of a perfect high-k/TI interface is a must to realize real device applications based on TI FETs. In particular, the truly attractive property of TI as a channel material for device applications is its surface channel with high carrier mobility and velocity. Any formation of top-gate dielectric on semiconductors cannot be as important as on TI since the conducting channel is on the surface.

In conclusion, we have investigated ALD high-k oxide formation on Bi_2Te_3 as a top-gate dielectric. AFM studies reveal the feasibility of direct ALD of high-k dielectrics on this layered material. Electrical characterization shows a pronounced modulation by both top-gate and back-gate with the highest modulation of 76.1% achieved with simultaneous dual gate control. However, at this point, the top-gate modulation is not as effective as the back-gate modulation at the same electrical field due to the degraded interface between the ALD dielectric and the TI. Further studies on protecting the TI surface during ALD dielectric formation are on-going.[21–23]

The authors would like to thank X. Xu, C. Liu, G. Q. Xu, Y.P. Chen, A.T. Neal, and N. Conrad for valuable discussions and E. Milligan, W.J. Qian, J.F. Tian, and M. Xu for technical assistance. The work is supported by DARPAMESO program.

[1]M. Z. Hasan and C. L. Kane, Rev. Mod. Phys. **82**, 3045 (2010).
[2]C. L. Kane and E. J. Mele, Phys. Rev. Lett. **95**, 146802 (2005).
[3]H. Zhang, C. X. Liu, X. L. Qi, X. Dai, Z. Fang, and S. C. Zhang, Nature Phys. **5**, 438 (2009).
[4]J. Moore, Nature Phys. **5**, 378 (2009).
[5]L. Fu and C. L. Kane, Phys. Rev. B **76**, 045302 (2007).
[6]D. X. Qu, Y. S. Hor, J. Xiong, R. J. Cava, and N. P. Ong, Science **329**, 5993 (2010).
[7]T. Zhang, P. Cheng, X. Chen, J. F. Jia, X. Ma, K. He, L. Wang, H. Zhang, X. Dai, Z. Fang, X. Xie, and Q. K. Xue, Phys. Rev. Lett. **103**, 266803 (2009).
[8]D. Teweldebrhan, V. Goyal, and A.A. Balandin, Nano Lett. **10**, 1209 (2010).
[9]F. Xiu, L. He, Y. Wang, L. Cheng, L. T. Chang, M. Lang, G. Huang, X. Kou, Y. Zhou, X. Jiang, Z. Chen, J. Zou, A. Shailos, and K. L. Wang, Nature Nanotech. **6**, 216 (2011).
[10]H. Steinberg, D. R. Gardner, Y. S. Lee, and P. J. Herrero, Nano Lett. **10**, 5032 (2010).
[11]S. Cho, N. P. Butch, J. Paglione, and M. S. Fuhrer, Nano Lett. **11**, 1925 (2011).
[12]K. S. Novoselov, D. Jiang, F. Schedin, T. J. Booth, V. V. Khotkevich, S. V. Morozov, and A. K. Geim, Proc. Natl. Acad. Sci. **102**, 10451 (2005).
[13]W. Kullmann, J. Geurts, W. Richter, N. Lehner, H. Rauh, U. Steigenberger, G. Eichhorn, and R. Geick, Phys. Stat. Sol. B **125**, 131 (1984).
[14]W. Richter, H. Kohler, and C. R. Becker, Phys. Stat. Sol. B **84**, 619 (1977).
[15]V. Russo, A. Bailini, M. Zamboni, M. Passoni, C. Conti, C. S. Casari, A. L. Bassi, and C. E. Bottani, J. Raman Spectrosc. **39**, 205 (2008).
[16]L. M. Goncalves, C. Couto, P. Alpuim, A. G. Rolo, F. Völklein, and J. H. Correia, Thin Solid Films **518**, 2816 (2010).
[17]Y. Xuan, Y. Q. Wu, T. Shen, M. Qi, M. A. Capano, J. A. Cooper, and P. D. Ye, Appl. Phys. Lett. **92**, 013101 (2008).
[18]X. Wang, S.M. Tabakman, and H. Dai, J. Am. Chem. Soc. **130**, 8152 (2008).
[19]Y. Xuan, Y.Q. Wu, and P.D. Ye, IEEE Electron Devices Lett. **29**, 294 (2008).
[20]P. Walker and W. H. Tarn, *CRC Handbook of Metal Etchants* (CRC, Culver City, CA, 1990), p.163.
[21]D. Kong, J. J. Cha, K. Lai, H. Peng, J. G. Analytis, S. Meister, Y. Chen, H.-J. Zhang, I. R. Fisher, Z.-X. Shen, and Y. Cui, e-print arXiv:1102.3935v1 (2011).
[22]D. Kim, S. Cho, N.P. Butch, P. Syers, K. Kirshenbaum, J. Pagolione, and M.S. Fuhrer, e-print arXiv:1105.1410v1 (2011).
[23]H. M. Benia, C. Lin, K. Kern, and C.R. Ast, e-print arXiv:1105.2664v1 (2011).